

## Supporting Information

Poly(3-hexylthiophene) grains synthesized by  
solvent-free oxidative coupling polymerization  
and their use as light-responsive liquid marble stabilizer

*Hiroki Inoue<sup>†</sup>, Tomoyasu Hirai<sup>†,\*</sup>, Haruka Hanochi<sup>‡</sup>, Keigo Oyama<sup>†</sup>, Hiroyuki  
Mayama<sup>§</sup>, Yoshinobu Nakamura<sup>†,‡</sup>, Syuji Fujii<sup>†,\*</sup>*

<sup>†</sup>Department of Applied Chemistry, Faculty of Engineering  
Osaka Institute of Technology, 5-16-1 Omiya, Asahi-ku Osaka 535-8585, Japan.

<sup>‡</sup>Nanomaterials Microdevices Research Center, Osaka Institute of Technology  
5-16-1 Omiya, Asahi-ku Osaka 535-8585, Japan.

<sup>‡</sup>Division of Applied Chemistry, Graduate School of Engineering  
Osaka Institute of Technology, 5-16-1, Omiya, Asahi-ku, Osaka 535-8585, Japan.

<sup>§</sup>Department of Chemistry, Asahikawa Medical University, 2-1-1-1 Midorigaoka-  
Higashi, Asahikawa 078-8510, Japan.

Corresponding Authors

\*(S. Fujii) Email: [syuji.fujii@oit.ac.jp](mailto:syuji.fujii@oit.ac.jp)

\*(T. Hirai) Email: [tomoyasu.hirai@oit.ac.jp](mailto:tomoyasu.hirai@oit.ac.jp)

### **Light-controlled movement**

A near-infrared (NIR) laser dot (808 nm; spot diameter, 1 mm  $\times$  5 mm; output power,  $\sim$ 200 mW) was manually irradiated sideways onto the LMs, aiming for three-phase contact, using an NIR laser pointer (Hikari, Inc). Accurate laser positioning for the three-phase contact was difficult to achieve by manual positioning, which caused fluctuation in the velocity and acceleration of LM locomotion. To simplify aiming toward the LM, an NIR laser detection sheet was placed underneath the Petri dishes and acrylic glass (IR sensor card 800-1600 nm, LDT-008, Laser Components GmbH, Olching, Germany). (The visible laser dot stemmed from the laser detection sheet, which was underneath the water bath. Whenever the laser light did not irradiate the LM, it was converted into visible light by irradiation of the laser detection sheet. The shift in perspective of the visible laser dot and the liquid marble results from the upper-back-side illumination of the LM and the height difference between the LM floating on the water bath and the laser detection sheet.) A digital video camera (Sony Handycam HDR-CX270 V; 30 $\times$  optical zoom lens, Sony Co., Tokyo, Japan) was used to record movies and photographic images of the LMs, and their locomotion was recorded using a digital camera (Ricoh G700SE; 5.0 $\times$  optical zoom lens, Ricoh, Tokyo, Japan).

### **Software**

The movies were analyzed using commercial software (Keyence VW-9000 MotionAnalyzer, Keyence, Osaka, Japan) to determine the velocity, acceleration and applied force of the LMs. Using this software, we first determined the position of the center of mass of the objects in each frame,  $r(t)$ . We then obtained the finite difference in the position (displacement),  $\Delta r(t)$ , from the time course of  $r(t)$  and the velocity  $v(t) =$

$(\Delta r(t)) / \Delta t$ , where  $\Delta t$  is the video rate (1/30 s). From the finite difference in  $v(t)$ , we obtained  $\Delta v(t)$ , the acceleration  $a(t) = (\Delta v(t)) / \Delta t$ , and the force  $F(t) = ma(t)$ , where  $m$  is the mass of the object. We thereby evaluated the velocity, acceleration and force of the LMs.

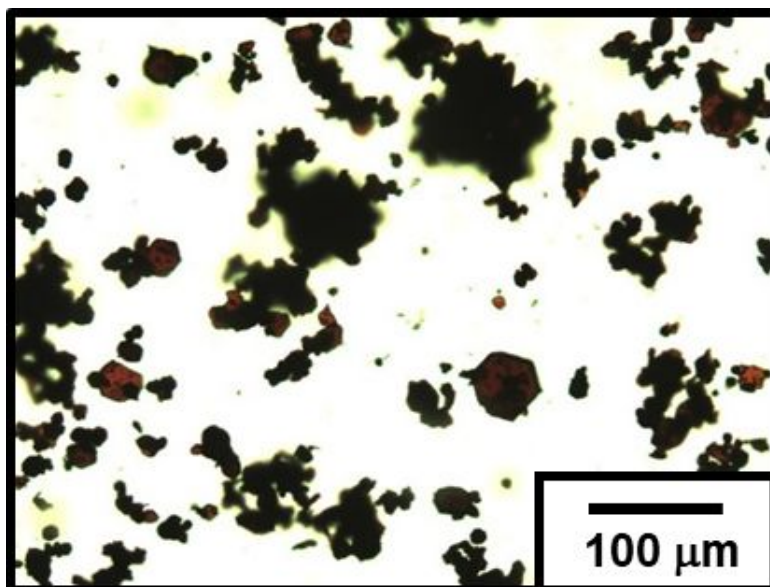


**Figure S1.** Stereoscopic microscopy image of  $\text{FeCl}_3$  oxidant particles.

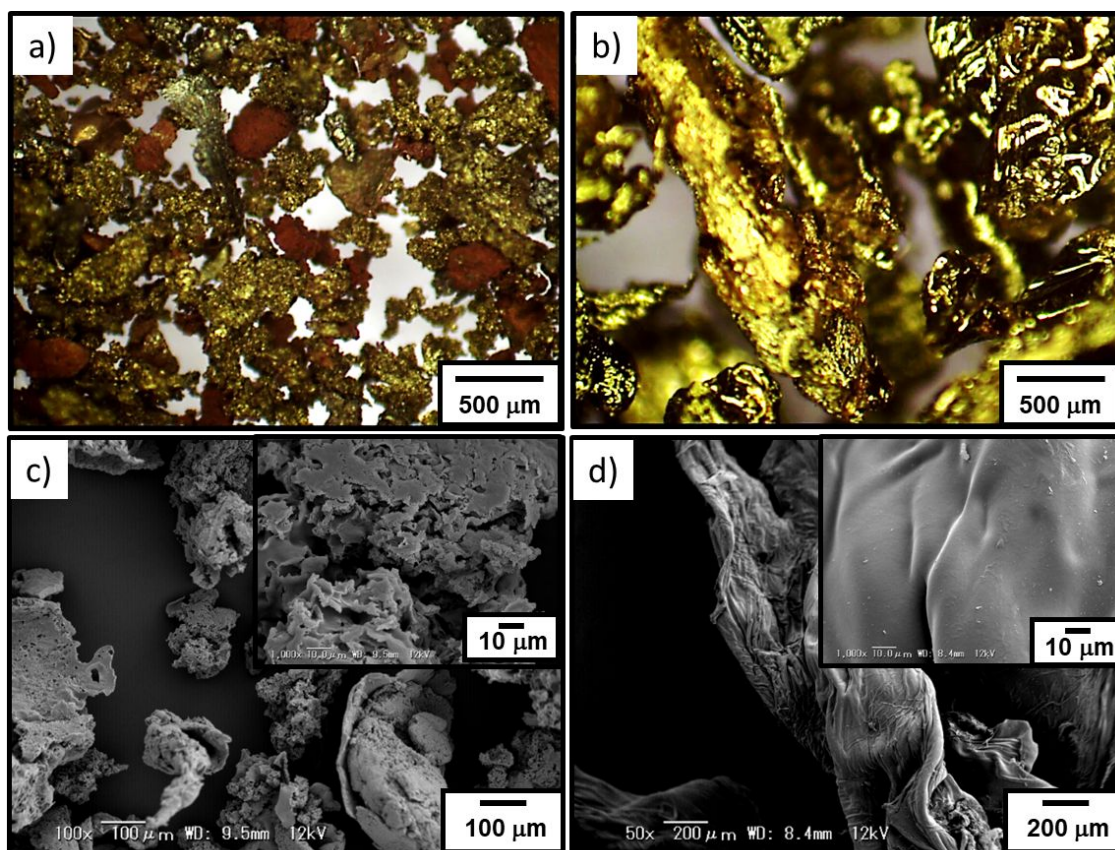


**Figure S2.** a, b) Stereoscopic and c, d) SEM images of a, c) P3HT materials synthesized by  $\text{CHCl}_3$  solution method (P3HT(solution)) and b, d) commercially purchased P3HT (P3HT(commercial)). The insets in the figures show the magnified SEM images.

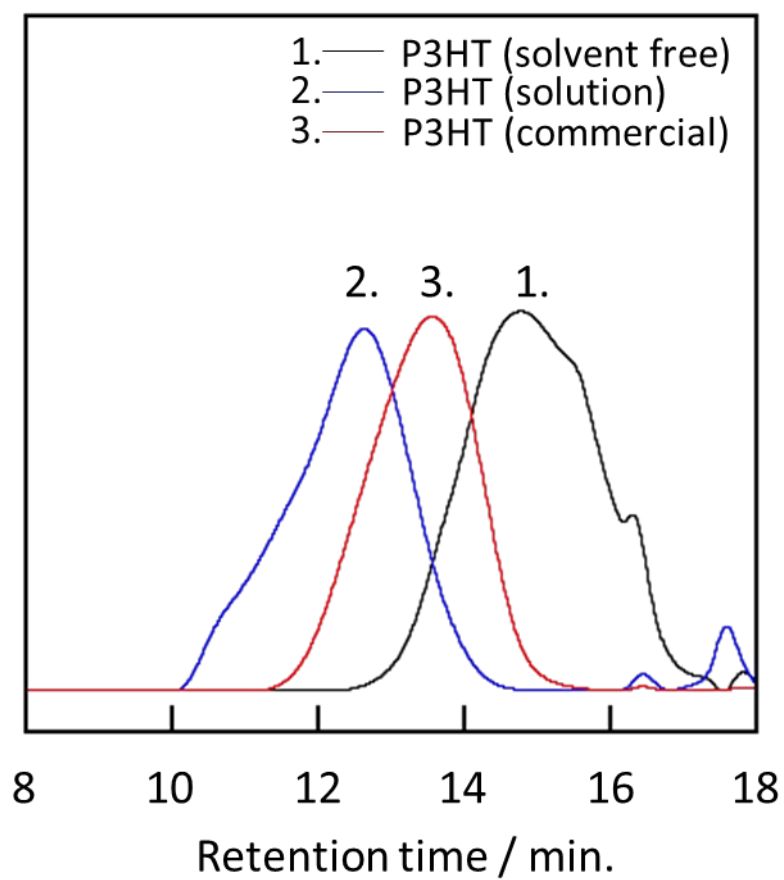


**Figure S3.** SEC curves of 1) P3HT(solvent free), 2) P3HT(solution) and 3) P3HT(commercial).

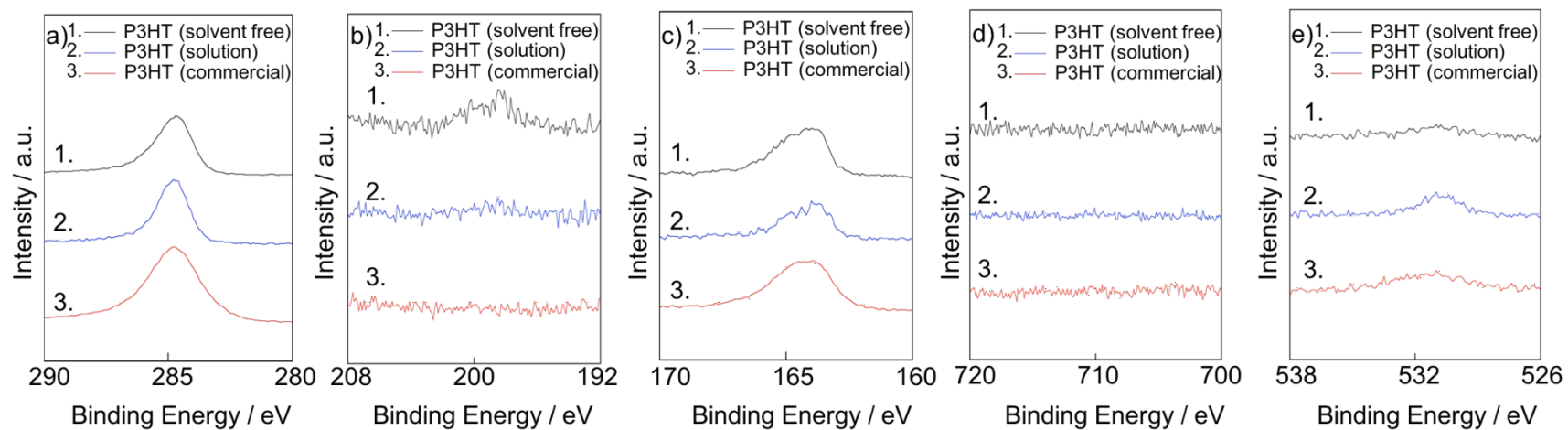


**Figure S4.** XPS high resolution spectra of a) C<sub>1s</sub>, b) Cl<sub>2p</sub>, c) S<sub>2p</sub>, d) Fe<sub>2p</sub>, and e) O<sub>1s</sub> for 1) P3HT(solvent free), 2) P3HT(solution) and 3) P3HT(commercial).

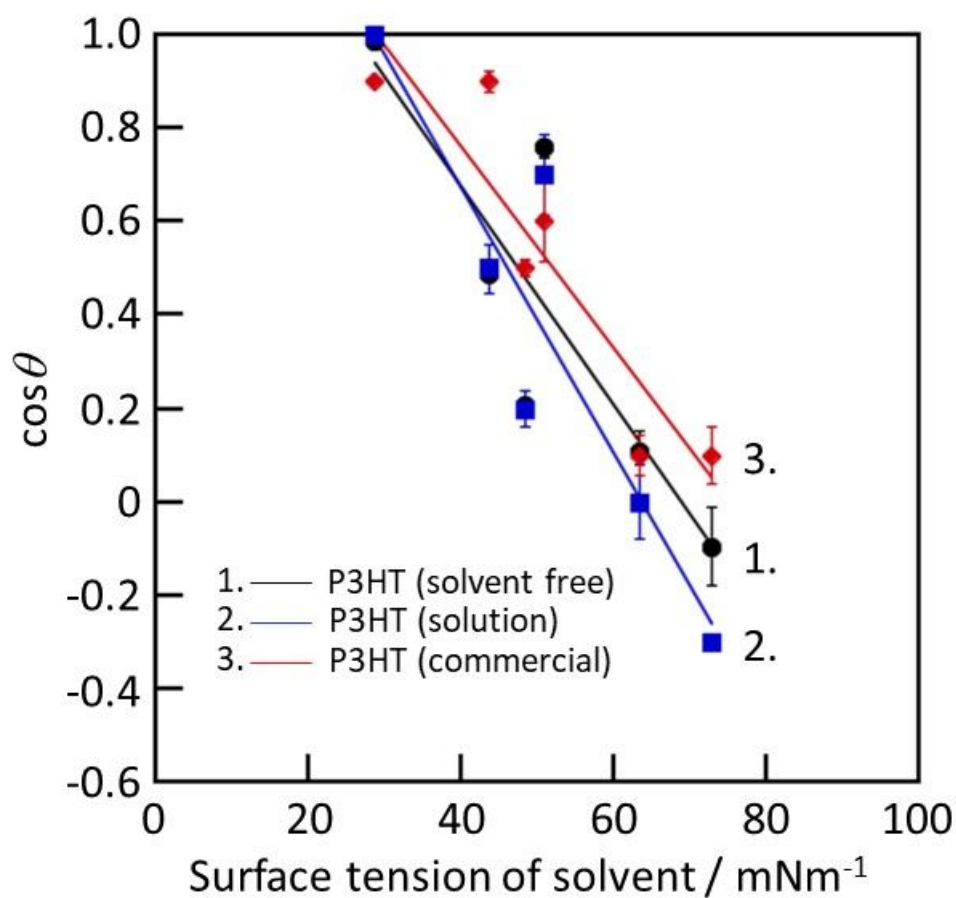


**Figure S5.** Zisman plots for P3HT(solvent free), P3HT(solution) and P3HT(commercial). The critical surface tension  $\gamma_c$  were determined to be 25.0  $\text{mNm}^{-1}$ , 28.2  $\text{mNm}^{-1}$ , and 30.3  $\text{mNm}^{-1}$  for P3HT(solvent free), P3HT(solution) and P3HT(commercial), respectively.



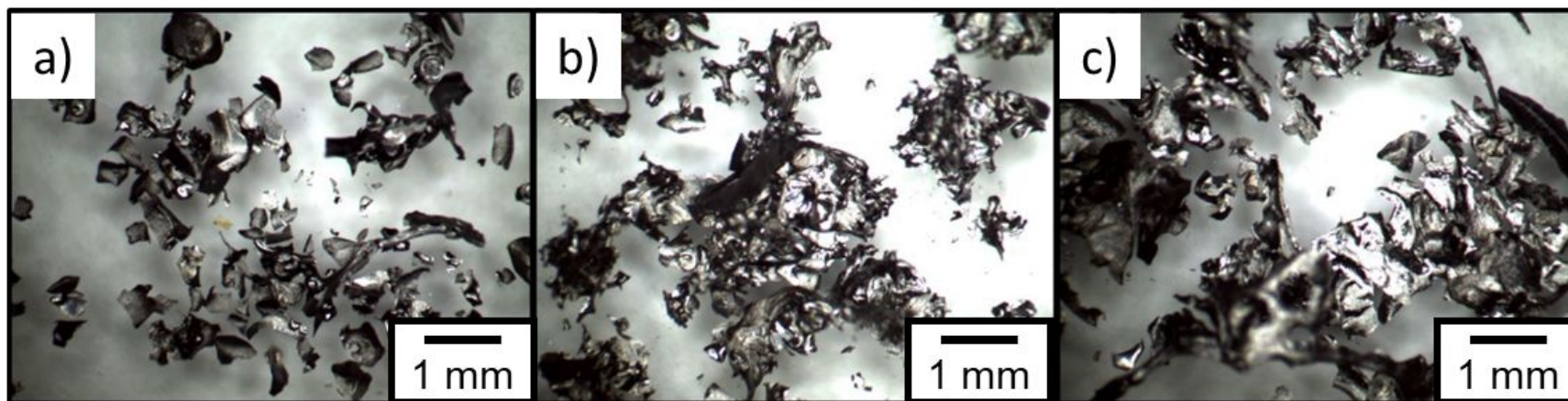


**Figure S6.** Optical microscopy images of 1) P3HT(solvent free), 2) P3HT(solution) and 3) P3HT(commercial) after TGA studies



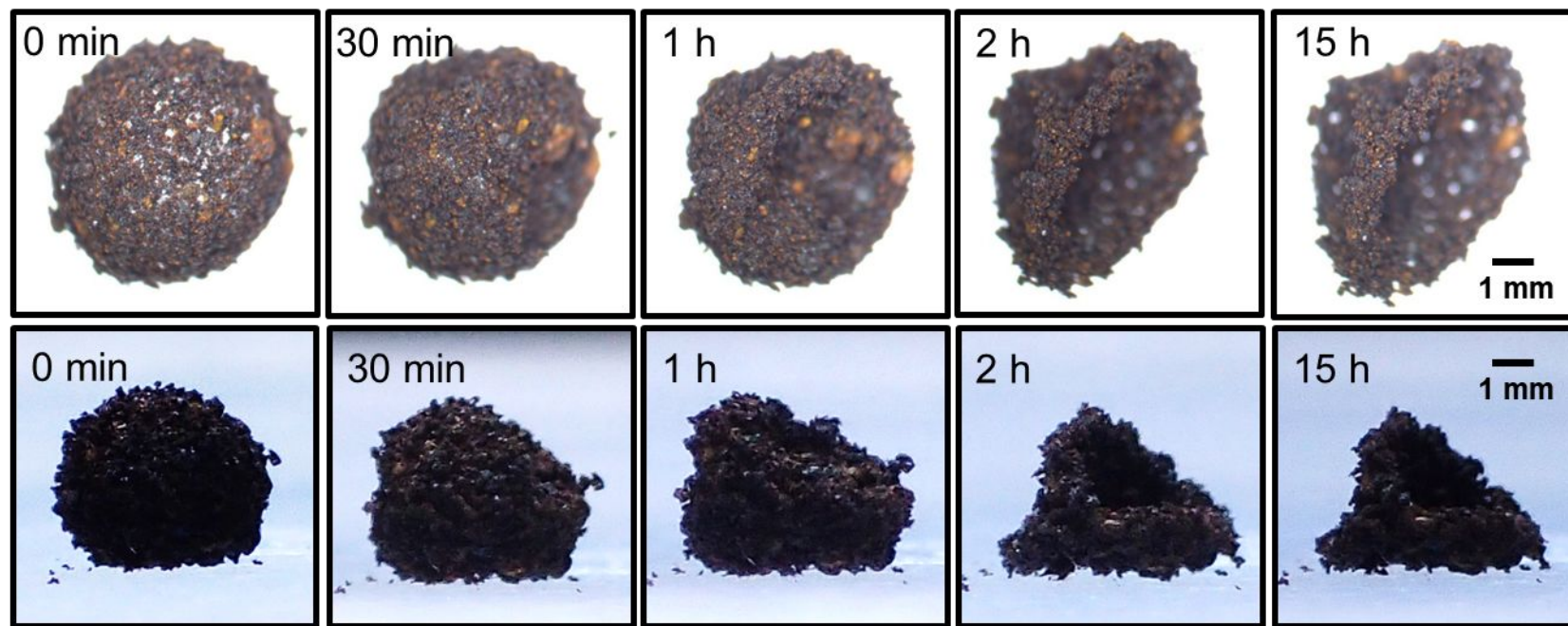


**Figure S7.** Digital photographs illustrating the effect of water evaporation on the gradual deformation and eventual collapse of a liquid marble after being placed on glass slide at 25°C and 54 %RH: (Upper row) top view and (Lower row) side view. Water volume is 15  $\mu\text{L}$ .